ELSEVIER

Journal of Membrane Science 161 (1999) 247–261

journal of
MEMBRANE
SCIENCE

Variance of streaming potential measurements

Michelle Chapman Wilbert[a,1], Saied Delagah[b], John Pellegrino[b,*]

[a] *US Bureau of Reclamation, Water Treatment Engineering and Research, MS D-8230, PO Box 25007, Denver, CO 80225, USA*
[b] *National Institute of Standards and Technology, 325 Broadway, Boulder, CO 80303, USA*

Received 9 November 1998; received in revised form 22 March 1999; accepted 23 March 1999

Abstract

We evaluated sources of variance in the measurement of the surface streaming potential of flat sheet specimens of cellulose di/triacetate membranes with a commercial electrokinetic analyzer. Two measurement methods were evaluated: the instrument's standard operating procedure, which continuously ramps the flow past the specimen, and a modified procedure that periodically stepped the flow rate and required manual calculation of zeta potential from the archived pressure and streaming potential data. Our study indicated that the kinetics of equilibration between electrolyte, electrodes, and membrane has the greatest impact on measurement uncertainty of any method used. An optimized protocol was developed for each method and the type A uncertainty (standard deviation) for the data collected using the optimized, modified procedure was one-third the value obtained using the optimized, standard procedure. © 1999 Elsevier Science B.V. All rights reserved.

Keywords: Cellulose acetate membrane; Streaming potential; Zeta potential; Membrane potentials

1. Introduction

Characterization of membrane surface charge by streaming potential measurements has become an increasingly popular descriptor to correlate against differences in fouling and solute rejection behavior [1–5]. Additionally, measurement of changes of streaming potential can be used to assess the results of a variety of surface modification strategies [2–4,6]. Most often, streaming potential measurements are made over a range of electrolyte velocities and these data are then used to calculate the zeta potential (ZP). In the measurements, the electrolyte fluid's conductivity, pH, and composition can be varied to further map the electrokinetic nature of the surface under study [3,7–13].

Electrokinetic measurements are being made on membranes that cover the separations spectrum from microfiltration [7,8,10] to ultrafiltration [2,6,9,10,13] to nanofiltration and reverse osmosis [1,3–5,11,12]. Therefore, examples of streaming potential measurements made either by flow through the pores of a membrane [1,2,7–10,13] or across the surface [3,4,6,11,12] are available.

Some prior studies have included some statements and results that address uncertainty in individual measurements and data scatter. The latter has mostly been assigned to sample–sample variability. Keesom et al. [8] reported the zeta potential of polycarbonate track-etched microfilters. Their data had uncertainties of as much as ±100% that they assigned to membrane variability and not to the precision of their apparatus.

---

*Corresponding author. Tel.: +1-303-497-3416; fax: +1-303-497-5224; e-mail: jjp@boulder.nist.gov

[1] mchapman@do.usbr.gov

PII: S0376-7388(99)00117-9

Kim et al. [10] reported a ±10% maximum uncertainty for repeated measurements on the same membrane sample (polysulfone) under the same experimental conditions, and somewhat larger variability within different samples from the same membrane batch.

Childress and Elimelech [11,12] used an instrument similar to the one with which we performed our studies. They reported that repeated measurements on two different samples of the same membrane (either cellulose acetate blend or aromatic polyamide) varied by ±10% in most cases. They also suggested that only new membrane samples be used every day and storage overnight in electrolyte solution caused uncertainties greater than ±20%. An equilibration time of only 30 min for salt adjustment and 10 min for pH changes was recommended.

Based on our own experiences [3,4], that are summarized in the background material following, we felt that it would be useful to report the details of an investigation of sources of streaming potential measurement uncertainties. In that context we chose three different operating modes for measuring streaming potential on flat surfaces. The study used cellulose acetate blend reverse osmosis membranes, but the general techniques of the study and conclusions should be applicable to any flat surface, membrane or other.

2. Background

We used ZP measurements to characterize surface energy changes as part of a membrane surface modification study to promote fouling resistance in reverse osmosis (RO) and nanofiltration (NF) membranes [3,4]. In that study, cellulose di/triacetate (CA) and polyamide (PA) thin film composite membranes were treated with a variety of polyetheroxide-based surfactants, tested for permeability and NaCl rejection, then exposed to a fouling solution and retested. ZP, atomic force microscopy, and acoustic time domain reflectometry were evaluated for their potential to quantify changes in the membrane surface before and after surfactant treatment and fouling by adsorption. Of these methods the ZP measurement was the most capable of detecting differences between surface treatments.

During the surface modification study, ZP was measured for the various membrane samples (with and without surface treatments) in KCl solutions with conductivity ranging from 30 to 120 mS m^{-1} and pH ranging from 3 to 7. Due to the large number of samples, measurements were repeated only for the untreated CA (or PA) RO membranes. Fig. 1 illustrates a set of results for unfouled CA membranes (with and without surfactant treatments), and Fig. 2 illustrates the results for fouled membranes. It seemed clear that the fouled membranes provided a substantially different zeta potential profile than the virgin (untreated and unfouled) CA membranes. But the uncertainty in the replicate measurements on the virgin CA membrane was large enough to make any conclusions with respect to differences between it and the various surfactant-treated (but unfouled) membranes imprudent. The question of overall reproducibility needed to be addressed systematically.

While care was taken to set the instrument up in the same manner each day during the surface modification study, there were random variations in the temperature, pH, and conductivity due to equipment and environmental limitations. One data point (at a specific conductivity and pH) consisted of 10 replicate measurements that took approximately 10 min to complete. Atmospheric CO_2 dissolving into the electrolyte solution can cause the pH to drift and ZP could change by 5 mV for a change of ±0.1 in pH. Conductivity also changes slightly as acid or base was added to vary pH. Solution temperature was recorded but not actively controlled during the early part of the original study, and ambient temperature variations of ±3°C were noted during the summer. The effect of temperature on viscosity is taken into account by the software, but it may also affect other aspects of the potential measurement including the kinetic response at the electrodes. Further exploratory measurements indicated that a fairly detailed evaluation of sources of variance in ZP measurements would be appropriate. The initial phase of that evaluation is presented in this study.

3. Theory

Detailed discussions of electrokinetic phenomena can be found in a variety of references [14–16]. In

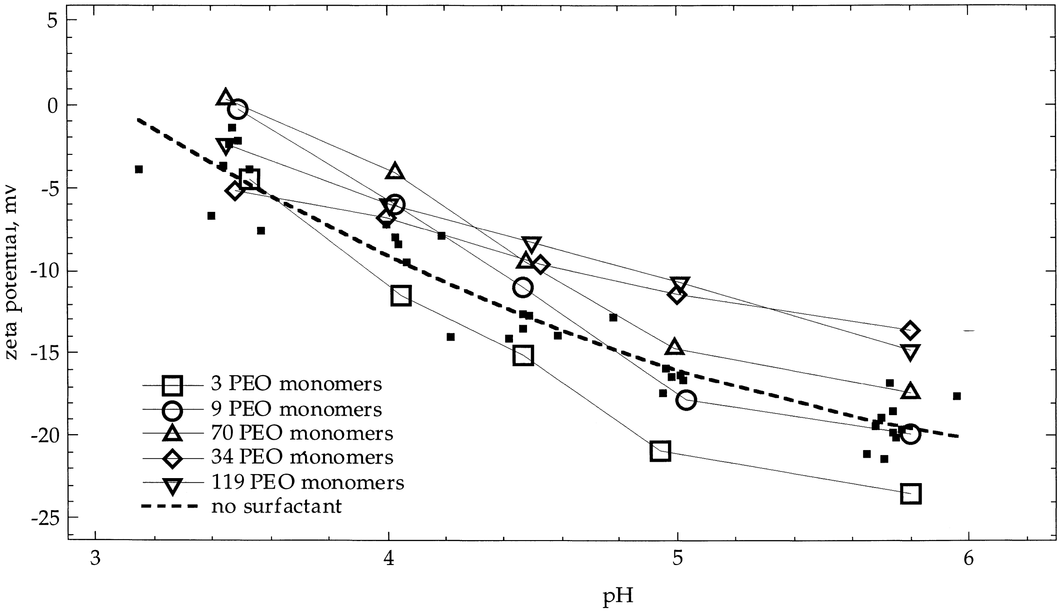

Fig. 1. Zeta potential against pH using KCl electrolyte, k=60 mS m^{-1}. Measurements are for new cellulose di/triacetate, reverse osmosis membranes that have been coated with polyethyleneoxide (PEO)-based surfactants (two different head groups – alkylphenol or polypropylene oxide) with varying monomer chain lengths. The (■) are replicates from several uncoated new membranes. The measurements were made using the instrument's standard operating procedure.

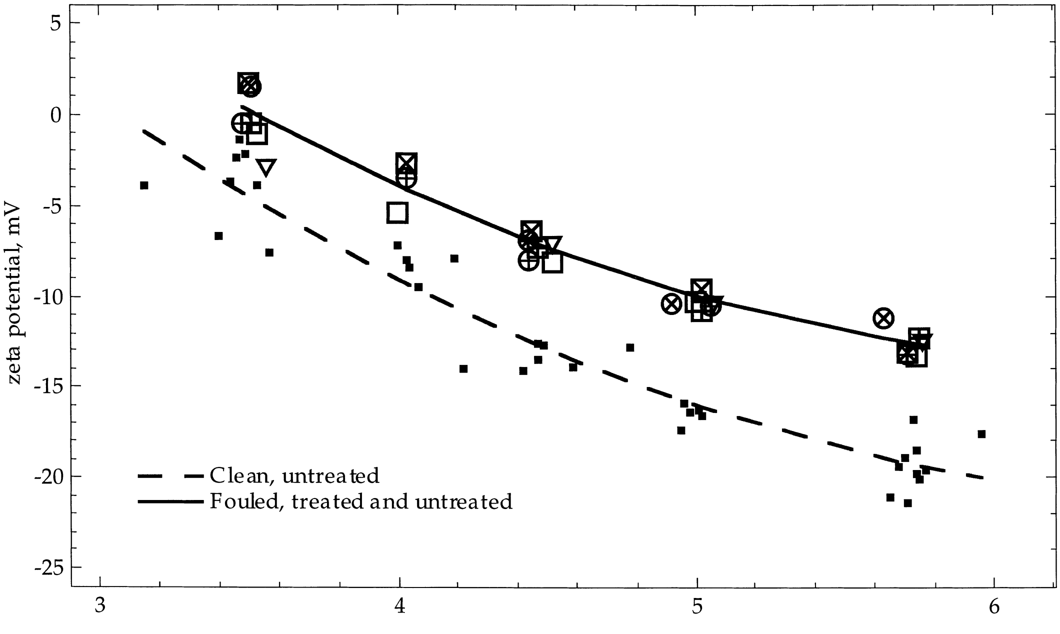

Fig. 2. Zeta potential against pH using KCl electrolyte, k=60 mS m^{-1}. Measurements are for the uncoated and each of the surfactant coated CA membranes after exposure to our standard fouling solution. The data (■) from uncoated, unfouled membranes are presented for comparison. The measurements were made using the instrument's standard operating procedure.

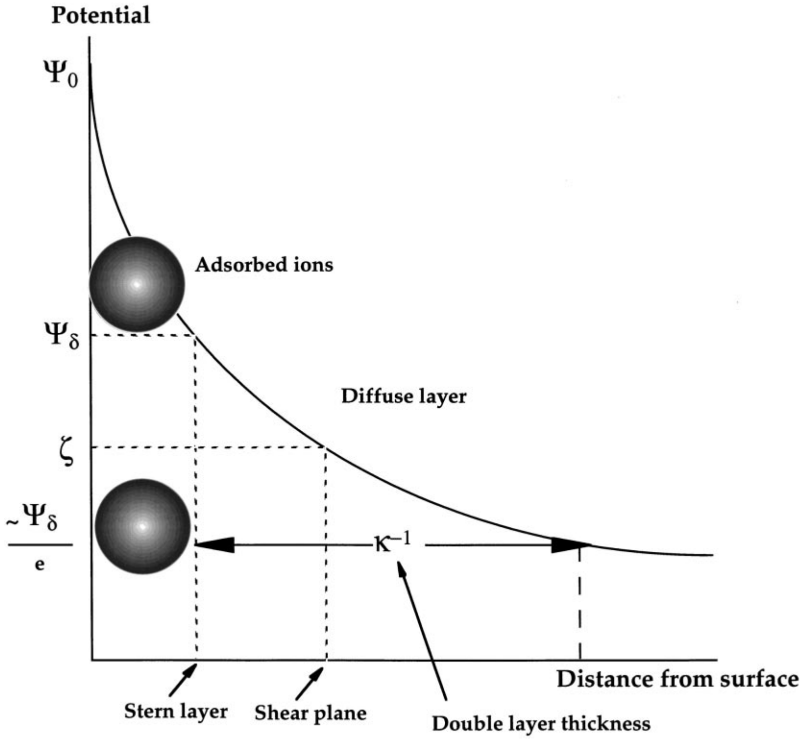

Fig. 3. Schematic representation of the change in surface potential with distance.

general terms, electrokinetic phenomena are reflections of the interaction of dissolved charges (ions) with a ''fixed'' surface charge density leading to a ZP at the plane of hydrodynamic shear. In fact, even when a neutral surface is exposed to an ionic solution, a difference in affinity of hydrated ions for the surface (due to surface free energy) can cause one type (charge) of ion to become more closely associated with the surface [14,16]. In general, a double layer charge develops as shown schematically in Fig. 3. The ZP is the electrical potential at the distance from the surface where ions are free to move. It is measured by circulating an ionic solution past the surface and measuring the streaming potential caused by the movement (current) of the excess ions associated with the surface.

ZP was calculated using the method described by Fairbrother and Mastin [17] for flat sheet samples with insignificant surface conductivity. It is based on the Helmholz–Smoluchowski relationship:

$$\zeta = \frac{\Delta U \cdot \eta \cdot L}{\Delta P \cdot \epsilon\epsilon_0 \cdot A \cdot R}, \tag{1}$$

where ζ is zeta potential (mV), $\Delta U/\Delta P$ the change in streaming potential with pressure (mV Pa^{-1}), η the viscosity of the solution (Pa·s), L the channel length (m), ϵ_0 the permittivity of free space (8.854×10^{-12} C^2 J^{-1} m^{-1} or s m^{-1} Ω^{-1}), ϵ the dielectric constant of the solution, A the cross-sectional area (m^2) and R is ohmic resistance of the electrolyte and channel (Ω).

In the Fairbrother–Mastin approach it is assumed that the electrolyte solution, with conductivity k, carries most of the current and is used as an approximation of L·A^{-1}·R^{-1} for ionic solutions>10^{-3} M. This approximation is acceptable for the membrane materials evaluated and results in the following simplification where k is the specific conductance:

$$\zeta = \frac{\Delta U \cdot \eta \cdot k}{\Delta P \cdot \epsilon\epsilon_0}. \tag{2}$$

Examining Eq. (2) shows that there are many potential sources of uncertainty in the measurement that fall into one or more of three categories:

1. Changes in the solution affecting the viscosity and surface charge (such as temperature, pH, and conductivity).
2. Slight differences in instrument setup and operation that change the channel geometry and may have an effect on other parameters as well.
3. Differences in the membrane surface due to handling or manufacturing that will affect the membrane's surface energy.

In this study of the sources of ZP measurement variation, the solution conductivity, pH, and temperature were strictly controlled. Box, Hunter, and Hunter's method of experimental design [18] was used to test the effect of differences in instrument setup and operation on ZP variation. The complete experiment was repeated three times (with different pieces of the membrane material) to include variation due to material differences.

4. Methods and materials

4.1. Electrokinetic analyzer

Fig. 4(a) is a schematic diagram of the electrokinetic analyzer apparatus (EKA). The electrolyte solution is held in a jacketed reservoir kept at constant temperature with water circulated through a heating and cooling water bath. The external pH and conductivity sensors are placed in the electrolyte reservoir. Conductivity, temperature, pressure, and streaming potential are monitored with internal sensors. A computer file is created to operate the pump automatically. Values for the maximum pressure, flow direction, and number of pressure ramp cycles are specified in this run file. Each cycle results in a calculation of ZP, $\Delta U/\Delta P$, and the correlation coefficient for $\Delta U/\Delta P$. At the end of the run, when the specified number of cycles is complete, the results are averaged, and a standard deviation (s.d.) for the ZP is calculated.

4.2. Measurement cell and spacer materials

Fig. 4(b) is a schematic of the measurement cell. It has flow inlets cut into the top half and electrode ports on the sides. A compartment is etched out of the middle of the two halves to form a defined flow channel. Seven layers of spacers, washers, seals and membrane are sandwiched between the two halves: silicone rubber washer, membrane (active side down), p-film (a blend of paraffin wax and polyethylene) seal, teflon spacer, p-film seal, membrane (active side up) and silicone rubber washer. The flow inlet and outlet are cut from the upper washer, membrane and p-film using a template for precision. The center spacer also has the flow channel cut out and serves to define the cross-sectional area of the channel.

4.3. Instrument set-up

Every two months, the pH sensor was calibrated with pH 4 and 10 buffers, and checked with pH 7 buffer and the internal and external conductivity sensors were calibrated with standard conductivity solution (44.7 mS m^{-1}). Insignificant drift in the sensors was noted between calibrations. Before each day of testing, the system was rinsed with 2 l of DI water and flushed to displace the water in the system. Once the membranes were placed into the measurement cell, a ruler was used to position the electrodes to ensure consistent alignment. Electrolyte solution was circulated through the system for 30 min to rinse the membrane. The pH was adjusted with HCl and the conductivity was adjusted with a KCl solution. At the end of testing, the system was flushed with DI water once again.

4.4. Membrane preparation

New cellulose di/triacetate flat sheet membranes were used for this study as for the previous surface modification study. Membrane samples were cut to fit the measurement cell and then wetted in 60 mS m^{-1} KCl solution at pH 6 and stored in a refrigerator for the soaking time specified in the experimental design.

5. Measurement protocol

5.1. Preliminary screening test

Experimental design as described by Box et al. [18] is useful for evaluating the effects of many factors in a

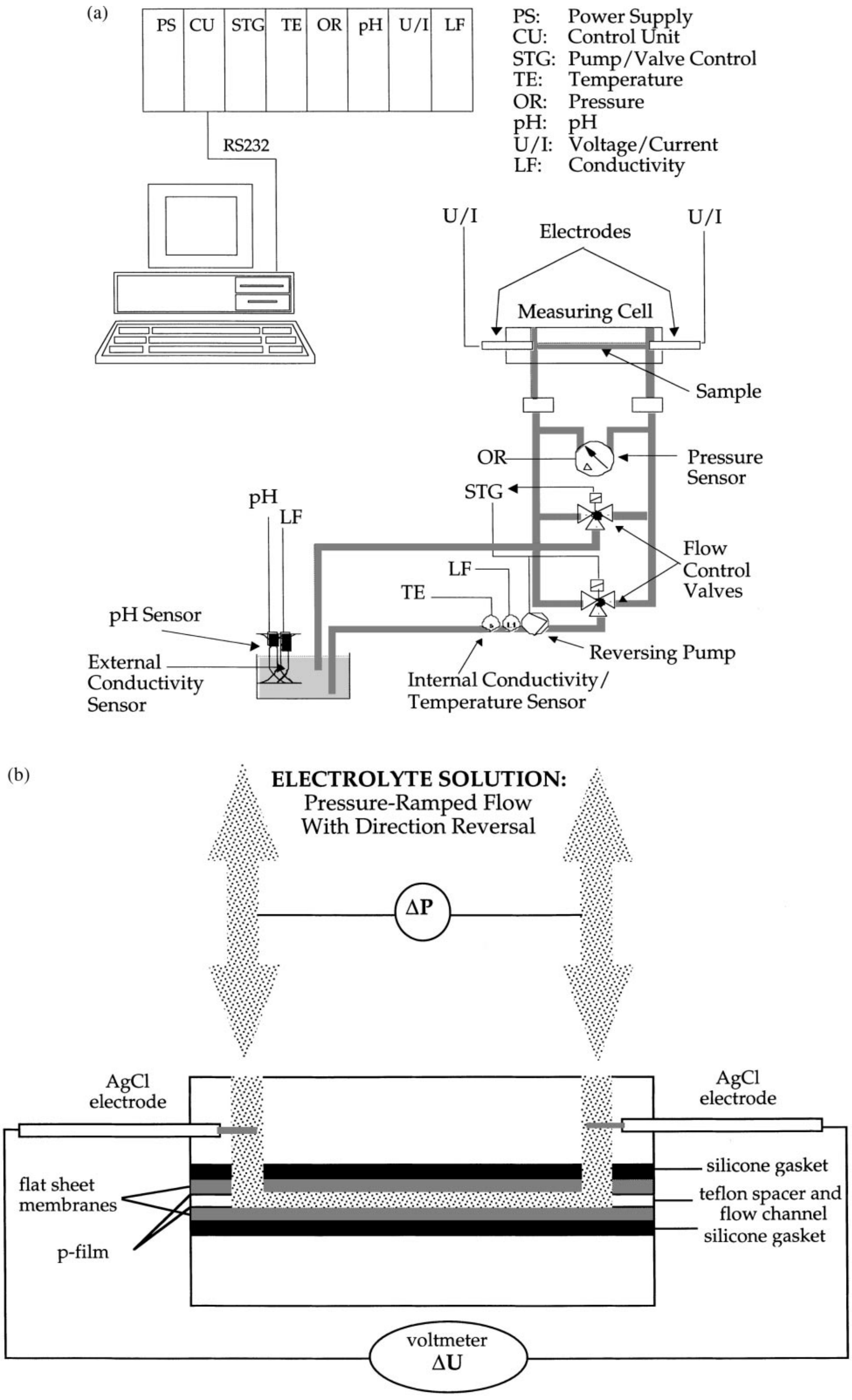

Fig. 4. (a) Flow and electrical diagram of an electrokinetic analyzer; (b) schematic of the measurement cell.

Table 1
Experimental design factors and levels

Design factor	Low level	High level
Maximum pressure	25 kPa	35 kPa
Number of pressure ramp cycles used in average for each ZP data point	3	5
Rinse time before measurement	30 min	45 min
Electrode position	Close (halfway into stream)	Far (just into the stream)
Soaking time before measurement	2 days	1 day

process without testing every combination. Each factor is tested at two levels to determine the effect of the level on a response variable. When each test is costly or time consuming, as ZP measurements are, a fraction of the whole design can be run as a screening tool to determine which factors and interactions are the most important in the process. A half fraction of a five-factor design with two levels was used to gauge the importance of EKA setup, operation and sample preparation factors. Table 1 lists the factors and two levels used in the preliminary experiments. The s.d. associated with the average ZP was used to evaluate improvement in method and the average ZP was used to estimate variation between membrane samples.

5.2. Alternative operating modes

After the measurements for the preliminary experimental design were completed, new software became available for the EKA that allowed archival recording of the real-time streaming potential data (such as is used in the automatic ZP calculation for each pressure ramp cycle). Having access to this raw data for off-line calculations made alternative operating modes possible.

In the normal pressure ramp mode (NM) – the basic technique used by the EKA instrument – the flow in the channel formed by the two membranes is continuously increased until the maximum set pressure is reached. Pressure drop across the channel is used as a surrogate for flow rate and the pressure "ramp" slope is fixed at 0.2 kPa s^{-1}. The instrument measures pressure and potential between the two electrodes (streaming potential) and determines the slope $\Delta U/\Delta P$ for use in the calculation of ZP with Eq. (2). Implicit in this mode is the assumption that the ion conductance around the electrodes is relatively instantaneous, and that the potential immediately establishes itself regardless of the inherent mass-transfer differences that result from changing flow rates and concentration gradients. To consider the effect on the ZP measurement uncertainty from faults in this assumption, we established an alternative protocol – pressure step mode (PSM). In this operating protocol we change the pressure in a stepwise fashion and allow the measured streaming potential to reach a constant value before making the next pressure step.

Fig. 5 presents measurements of the streaming potential at two pressure levels and in both flow directions using PSM. Note that it takes at least 50–60 s before a steady value of the streaming potential is obtained at a given pressure. In PSM we record the data, determine the constant streaming potential for each pressure, and calculate the ZP off-line.

We used two variations of the PSM method to investigate possible equilibrium destabilization resulting from a change in the flow direction. In the bi-directional PSM (BPSM) a measurement was taken with the pressure held at one level for each of the two flow directions. This yields two streaming potential data points – one at the positive ΔP and the other at the negative ΔP. This procedure was followed as the pressure level was incremented stepwise from the minimum to the maximum. Then a last pair of duplicate points were taken at a low ΔP to check for any significant hysteresis. For the uni-directional PSM (UPSM) the pressure was decremented from maximum to minimum without changing flow direction until the measurement at the lowest pressure step was completed. Then the flow was reversed and the pressure was incremented to the maximum again. Fig. 6 is a graphical representation of the three different measurement modes: NM, BPSM, and UPSM. The vertical axis is used to portray flow direction with positive pressure values representing right to left flow and negative pressure values representing the reverse flow

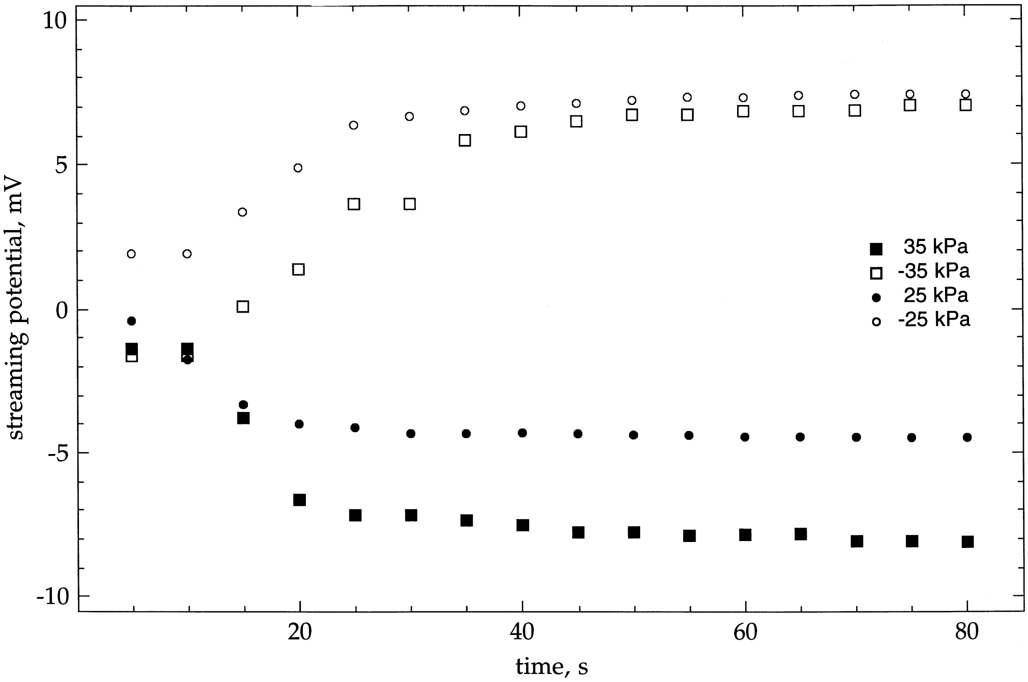

Fig. 5. Sample pressure step mode (PSM) streaming potential measurements against time for two pressures in both forward and reverse directions. Negative pressure indicates reverse flow.

direction. Time, on the x-axis, is proportional to the length of time the sample is subjected to that pressure and flow direction. The span of time covered for each mode of measurement is proportional to the time required to produce one calculated $\Delta U/\Delta P$ (or ZP). For the NM this single calculated ZP is the result of averaging the ten measurements (or five cycles) depicted in the figure. The UPSM also had the result of shortening the time required for a ZP data point using PSM.

To illustrate the data characteristics further, Fig. 7 shows representative ZP measurements from four series of NM measurements. There are three series of ten sequential ramps and one with six sequential ramps. (Note: Fig. 6 illustrates the pressure magnitude and flow direction vs. time history for one series of ten sequential ramps using NM.) Every sequential pair of ramps (one in '+' flow direction and the other in the '−' flow direction) is considered a cycle. A cycle is the minimum number of measurements needed to cancel the differences between the ZP values resulting from the forward and reverse observations due to asymmetry between the electrodes. Electrode asymmetry causes similar differences in the absolute value of streaming potential measurements in different directions using either of the PSM modes. The differences are cancelled out when the series of NM observations is averaged together to produce one data point and when equilibrium is established in PSM mode. The latter results in a distinctly linear relationship between streaming potential and pressure as shown in Fig. 8.

Fig. 8 is an example of the streaming potential against pressure (negative sign on pressure again indicates a change in flow direction) gathered using UPSM with data collected every 20 s for 300 s. We frequently observed a continuous upward drift in the absolute value of the streaming potential (see, for example, the data for 35 kPa in Fig. 5), which we were not able to eliminate.

5.3. Full factorial experimental design

A full factorial design with four factors, two levels each, and three separate material samples for each set of conditions was run to get an absolute evaluation of the significant factors identified in the preliminary

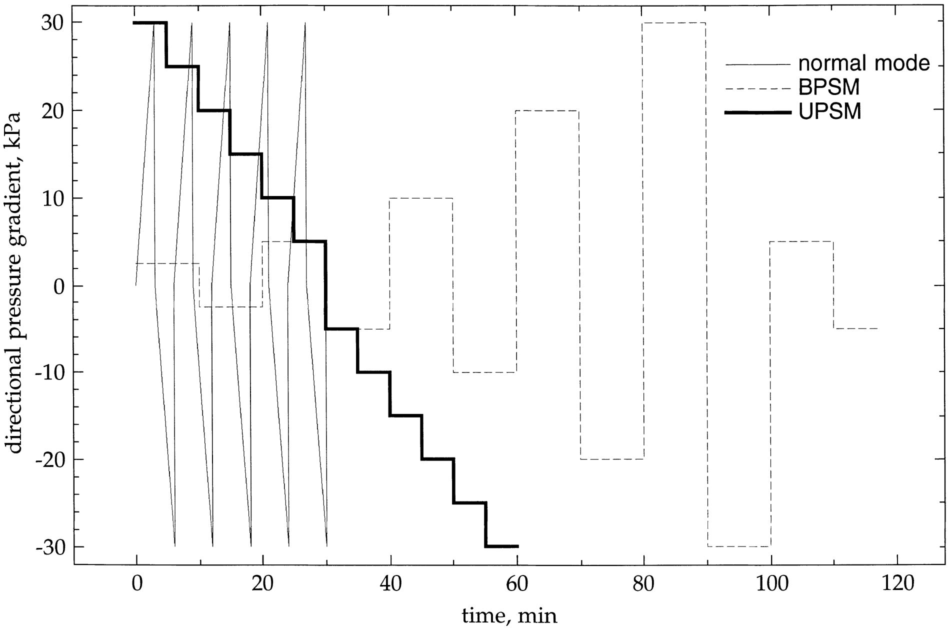

Fig. 6. The pressure magnitude and flow direction versus elapsed time history for the three different modes of operation. Negative pressures indicate reverse flow direction, not vacuum. In normal mode (NM), pressure is ramped to the maximum then flow is stopped, its direction is reversed and the pressure is ramped to the maximum in the opposite direction. Pairs of forward and reverse cycles can be repeated up to five times lasting 5–7 min each. In bidirectional pressure step mode (BPSM) the pressure is held constant in one direction for 10 min then flow is reversed and the same pressure is maintained in the opposite direction. Pressure is increased stepwise to the maximum. Unidirectional pressure step mode (UPSM) is similar to BPSM except that measurement is initiated at the maximum flow rate (and pressure) in one direction and stepped downward before reversing flow and stepping upward in pressure to the maximum in the other direction.

design and the importance of the operating mode. A total of 48 membrane samples were tested for a total of 168 data points on the same material, under the same test solution (pH, ionic strength, and temperature) conditions. Table 2 lists the factors and levels used for the full design. In Table 2, the number of cycles means something different depending on whether it is NM or UPSM. Number of cycles for NM means the number of pairs of ZP measurements averaged for a single data point, and for UPSM one cycle yields a single ZP data point (for example, in Fig. 6 there are five cycles or ZP measurements for NM, and one cycle or ZP measurement for UPSM).

Table 2
Factors and levels considered in the full factorial design

Factor	Low level	High level
Maximum pressure	25 kPa	35 kPa
Number of cycles	2 (UPSM) or 3 (NM)	4 (UPSM) or 5 (NM)
Soaking time[a]	1 day	3 days
Mode	NM	UPSM

[a] Low and high levels are experimental design nomenclature and do not need to conform to lower or higher quantitative values.

5.4. Response variables

The s.d. associated with the average of the $\Delta U/\Delta P$ data and the average R^2 values for the linear $\Delta U/\Delta P$ relationships were used as the response variables for judging uncertainty. Each data point for this comparison is an average of the results for each of the cycles measured. For the NM observations, a forward and reverse flow pressure ramp were averaged together to produce one cycle. For example, a NM run with data for five forward and five reverse pressure ramps is five cycles. Therefore, the two response variables were (1) the s.d. associated with the average $\Delta U/\Delta P$ for those five data points and (2) the R^2 that was calculated for the linear fit for $\Delta U/\Delta P$ by the software. With PSM,

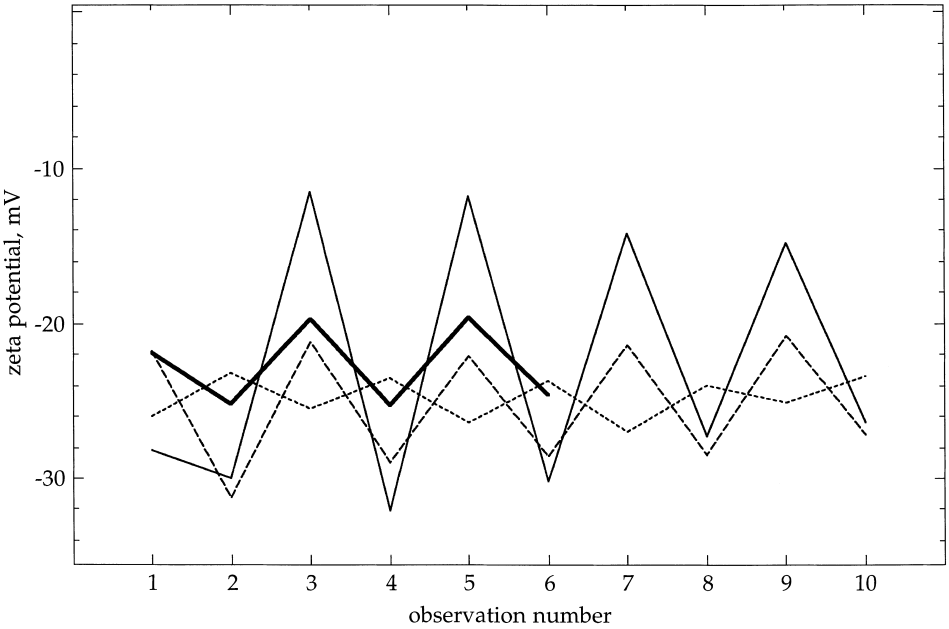

Fig. 7. Four series of consecutive NM measurements. The calculated ZP is plotted against observation number in the series. Gross differences between the forward and reverse measurements are due to asymmetry between the electrodes. Averaging the forward and reverse data for two consecutive measurements is the minimum requirement to cancel these differences and constitutes a cycle (two consecutive measurements – one in each flow direction.) A single ZP data point is the result of averaging all the cycles in a measurement series. This plot contains three series with five cycles and one series with three cycles.

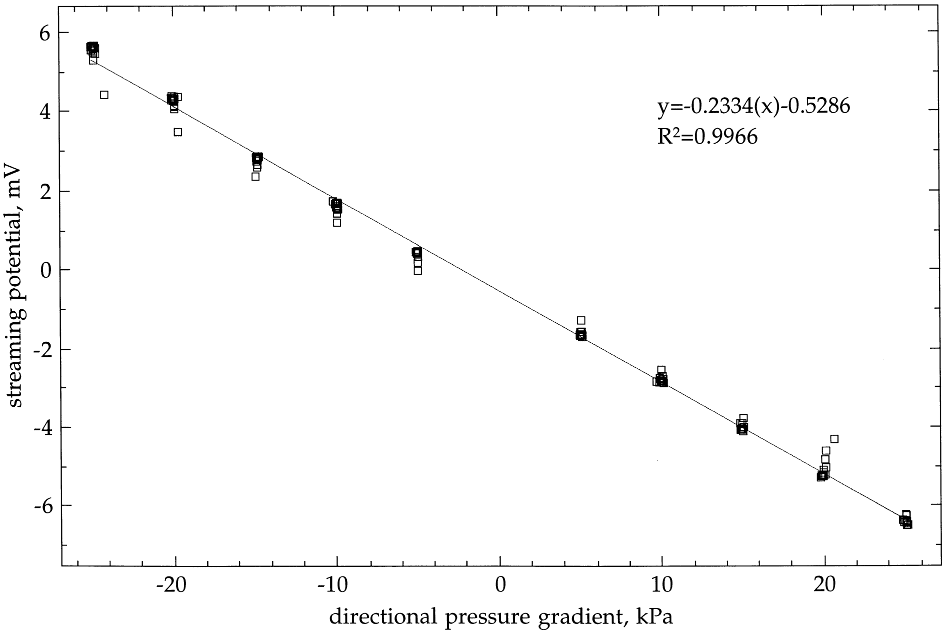

Fig. 8. Sample UPSM streaming potential measurements over a range of pressures. The potential data points tend to cluster and increase in absolute magnitude over time (total of 300 s of data collection at each pressure), especially at higher pressures. The intercept of the linear fit (0.5286) is the asymmetry voltage between the electrodes.

the data point would be simply the average of two or four cycles depending on the "number of cycles" factor level. The R^2 response value was the average R^2 for the set. With PSM, $\Delta U/\Delta P$ is calculated as the slope of the best-fit line for the change in streaming potential with pressure (for example, data in Fig. 8). Streaming potential and pressure values, as well as conductivity, temperature, and pH, are recorded at 5 s intervals over a period of 300 s and we can filter measurements that are taken during the initial period of rapid change (for example, the first 40 s in Fig. 5). The equilibrium values were used to calculate the response variables.

6. Results

6.1. Preliminary design

Fig. 9 is a matrix plot of the interactive effects between the factors used in the preliminary experimental design (Table 1). In a half fractional factorial design such as this, there is not enough data produced to compare more than two factors. The matrix plot should be read just as a mileage chart that gives distance between sets of cities. The factors are listed on the diagonal with their high and low levels just for reference. Across the top the high and low levels are listed for the factor at the bottom of that column. The vertical scale of the individual graphs is the average standard deviation of all the measurements taken under the particular set of conditions. The open circles represent the high level of the factor to the far left and the squares represent the low level. The other ordinate is its value along the top line (for example, the arrow identifies the point for a maximum P=35 and cycles=5). The actual value of the average standard deviations is not important at this stage. Only the relative differences are important. Strong interactions between two factors can be detected by a large difference between values at the high and low levels. For instance the inner electrode position (-1) consistently has a lower average standard deviation than the outer electrode position ($+1$) no matter what the other factors are. This indicates that the inner electrode position is best. A lower maximum pressure results in a lower average standard deviation when there are more cycles than a higher maximum pressure, but for fewer cycles the reverse is true. Longer soaking time consistently resulted in lower standard deviations. The "low" level for soaking time happens to be 2 days instead of 1, as would be more intuitive, but the actual value of the level is irrelevant as long as the the results are interpreted correctly.

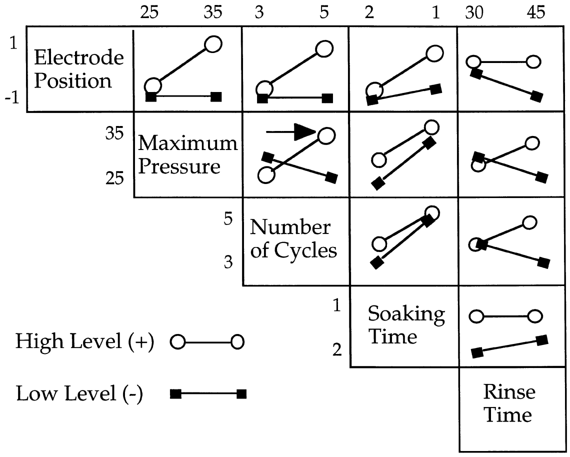

Fig. 9. Matrix plot of general effects of test factors on ZP standard deviation. Symbol style relates to levels of the row components. For example, the first row indicates how the electrode position interacts with maximum pressure, repeats, soaking time, and rinse time. The open circle is the high level interacting with the two levels of all the other factors (identified at the bottom of the columns with their values along the top line). For example, the arrow identifies the point corresponding to max P=35 and cycles=5. The filled squares are the low levels. The vertical axis for each graph is the standard deviation of all data taken with the particular pair of conditions indicated. The slope of each graph indicates the strength of interaction. Based on these results, the inner electrode position and shorter rinse time were chosen.

Based on the results of the preliminary design, the close electrode position and shorter rinse time were chosen for use in the full factorial and dropped as factors that might have a significant impact on measurement variation. Soak time, maximum pressure and the number of cycles were selected as factors most likely to produce uncertainty in ZP measurement.

6.2. Full factorial design

Table 3 lists the significant factors and interactions for each response variable with the probability that the factor or combination of factors has a statistically significant effect. The measurement conditions with

Table 3
Significant effects from the full factorial design with confidence levels greater than 90% (effects are based on analysis of 48 membrane samples with a total of 168 measurements)

Response	Factor interactions	(%) Probability
s.d. of $\Delta U/\Delta P$	Mode	99.9
	Cycles·soak·mode	95.7
	Cycles·soak	92.8
	Maximum P	92.6
	Cycles·mode	91.6
	Maximum P·cycles·mode	91.3
$\Delta U/\Delta P$	Cycles	91.2
Correlation for $\Delta U/\Delta P$	Cycles·mode	98.3

the lowest standard deviations are described in Table 4.

Fig. 10 shows cube plots for the s.d. of $\Delta U/\Delta P$ and the average value of $\Delta U/\Delta P$. Cube plots are helpful for visualizing interactions between three or more factors. Each dimension of a cube plot represents one factor. The corners of the cube are the low and high levels selected for that factor (the factor levels are in larger bold type). More than three factors can be represented by multiple sets of cubes such as used in Fig. 10. The cubes on the left are for NM data and the ones on the right are for UPSM data. In the top row, the values in the corners of the cubes are the average s.d. of $\Delta U/\Delta P$, and in the bottom row, the cube corners contain the average values of $\Delta U/\Delta P$. The values are the averages for measurements taken under the conditions at the intersection of factors. For instance, the 3.1 in the lower front left corner of the top left cube represents measurements taken using NM, with a maximum pressure of 25 kPa, three cycles and 1 day of soaking time. Its average $\Delta U/\Delta P=-0.21$ mV kPa^{-1}, with an s.d. of 3.1×10^{-2} mV kPa^{-1}. The number of observations going into that average depends on the number of cycles and mode as shown in Table 2. Since there were three membrane samples tested at each set of conditions, that particular point is the average of nine observations (three samples * three cycles). The conditions with the lowest s.d.'s are circled in the top right cube with their corresponding values of $\Delta U/\Delta P$ in the lower right cube.

Table 4
Measurement conditions with lowest standard deviations for UPSM and NM

	Unidirectional pressure step mode	Normal mode
Soaking time	3 days	Insignificant
Cycles	2	Insignificant
Maximum pressure	Insignificant	25 kPa

The only significant effect on the correlation for $\Delta U/\Delta P$ was the interaction between the number of cycles and the mode. There was a slightly higher correlation when more cycles were run using NM and fewer cycles using PSM. However, the average correlation coefficient for each of the 48 test conditions was greater than 0.97.

Fig. 11 is a plot of average $\Delta U/\Delta P$ vs. calculated ZP for each of the 48 membrane samples. The averages of observations taken under the best conditions (those in Table 4) are shown with uncertainty bars of three standard deviations. It is clear that a significant improvement in the uncertainty (as indicated by the s.d.) of the calculated ZP is obtained by using the optimum UPSM protocol. Similar average ZP values were obtained in both cases (−17.3 for the NM and −17.9 mV for the UPSM) but the s.d. for the ZP measurements was 2.7 mV for NM and 0.9 mV for UPSM using the optimum protocol.

7. Discussion

Besides the major conclusion about the overall operating protocol, a physical interpretation about the effects of the specific factors is helpful. Changing the electrode position (distance into the flow cell) affects the mass transfer around it and decreases the overall cell resistance. This probably affected the uncertainty of the measurements because (1) the outer position was more difficult to pinpoint each time and (2) the outer position did not place the electrode far enough into the flow channel to detect the voltage changes as sensitively. It was straightforward to mark the optimum inner position and make sure it was placed correctly for future measurements.

The longer presoaking period allowed the membrane to become more fully hydrated, and consequently, more uniform. The time could be shortened if the membrane material were exposed to the test

Cube Plot for ΔU/ΔP Standard Deviation (mV/kPa)*100 (data means)

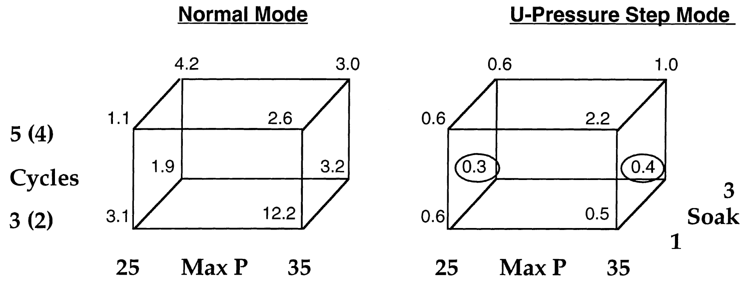

Cube Plot for ΔU/ΔP Average (mV/kPa) (data means)

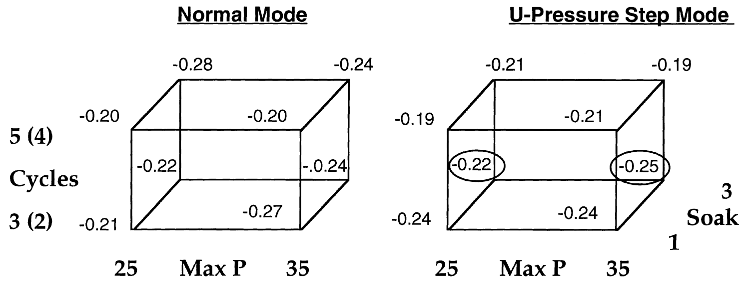

Fig. 10. The cube plots show interaction between maximum pressure (horizontal axis), soak time (depth axis), number of cycles (vertical axis). The two cube plots on the left side are for the NM of operation and the two on the right side are for the PSM. The two cube plots in the top row depict the s.d. in $\Delta U/\Delta P$ for all measurements at a particular set of conditions represented by the vertices and the mean value of $\Delta U/\Delta P$ is in the lower row. These values are placed at the vertices. The s.d. of $\Delta U/\Delta P$ is $\times 10^3$. The lower the s.d. in $\Delta U/\Delta P$ the better. A 1 day soak period with fewer repetitions using UPSM were the optimal operating conditions. This set of conditions is indicated by the circled values.

solution under pressure, but then there would be a greater chance for the membrane surface to be contaminated with colloidal substances.

Rinse time, maximum pressure, and the number of cycles reflect a variety of sources of uncertainty due to the entire system, including electrodes, electronics, the electrolyte solution, the flow system, and the membrane. The rinsing time between changes in operating conditions allows the system to reach a consistent starting point before the streaming potential is measured under new conditions. Thirty minutes was long enough for the purposes of this study since we were not changing solution conditions. It may be too short for examining the change in ZP with pH or conductivity (this issue will be examined in future work). Data such as those in Fig. 5 suggest that it might take longer for the system to reach equilibrium at higher pressures. If so, this would explain the lower standard deviations with lower maximum pressure. This problem could be overcome by continuing measurement until a plateau is reached rather than stopping after a particular time period. The number of cycles should not adversely affect the measurement uncertainty unless the method of reversing flow and changing pressure (in NM especially) is continually driving the system further toward or away from equilibrium. If the rinse and measurement times, in one direction at a single pressure, are long enough to attain equilibrium, then repeat measurements should only decrease uncertainty.

The results of the preliminary design showed that any factor that increased the length of the measurement time had a negative impact on the standard deviation of the ZP measurement. Higher maximum pressure and more measurement cycles both extend the measurement time and both resulted in higher

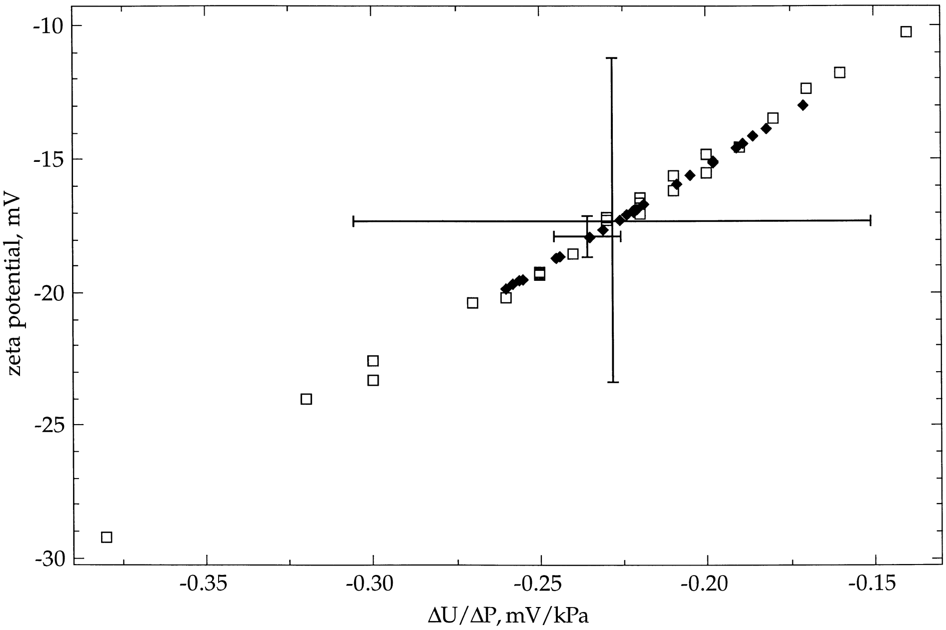

Fig. 11. The average $\Delta U/\Delta P$ for all 48 membrane samples are plotted against the calculated ZP. The (□) are using NM and (◆) are using UPSM. The two uncertainty crosses are at the mean of observations taken under the optimum operating conditions for the particular mode, with three standard deviations indicated.

standard deviations. The reason for this problem became apparent with the evaluation of different operating modes. With PSM and automatic data recording, the streaming potential takes up to 1 min to reach equilibrium. During NM operation, the pressure is constantly changing, so that the streaming potential never manages to reach equilibrium. The chances of getting measurements at exactly the same points of nonequilibrium are extremely small, as is reflected in the high variability of ZP measurements using NM.

With UPSM, only the soaking time and number of cycles had significant effects on measurement variation. The results in Table 4 indicate that a longer soaking time and fewer cycles decrease variability. Since each cycle took 80–100 min to complete, the adverse effect of a higher number of cycles is possibly due to adsorption of colloidal matter on the membrane and/or electrode surface from the instrument tubing. This hypothesis would need to be verified, but could possibly be corrected by using a filter on the reservoir. In Fig. 5 the potential had leveled off after approximately 60 s. Changes after that time may be due to drift in temperature, adsorption of colloidal matter, or just electronic noise.

8. Conclusions

This study demonstrates that measurement of the streaming potential of membrane materials can have a great deal of uncertainty associated with it, but it is possible to lower that uncertainty by optimizing the test protocol. The kinetics of equilibration between the electrolyte solution, the electrodes, and the membrane has the greatest impact on measurement uncertainty. Therefore operating with a continuously changing pressure (flow) is not recommended, even though it is the standard operating mode of some instruments. We have found that operating at several steps of pressure (flow), until a stable streaming potential is measured for each step, reduces measurement uncertainty considerably. The protocol we used in this study began at a flow pressure gradient of 30 kPa (flowing from right to left) which was decreased every 300 s in 5 kPa increments, and then the flow direction was reversed and the pressure gradient increased in 5 kPa increments until 30 kPa was reached. This procedure was done twice.

Furthermore, pre-equilibrating the membrane in the electrolyte solution for an extended period of time is also recommended. In the case study for cellulose acetate blend membranes and KCl a 3 day soak was optimum. The time required for establishing equilibrium is expected to change with membrane, solution conductivity, composition, and pH. Our future work will measure $\Delta U/\Delta P$ over a range of conductivity and pH with different membrane materials to provide guidance in developing further optimized measurement protocols.

References

[1] C. Combe, E. Molis, P. Lucas, R. Riley, M.M. Clark, The effect of CA membrane properties on adsorptive fouling by humic acid, J. Membr. Sci. 154 (1999) 73–87.

[2] A. Nabe, E. Staude, G. Belfort, Surface modification of polysulfone ultrafiltration membranes and fouling by BSA solutions, J. Membr. Sci. 133 (1997) 57–72.

[3] M. Chapman Wilbert, Enhancement of membrane fouling resistance through surface modification, Water Treatment Technology Program Report No. 22, US Bureau of Reclamation, 1997.

[4] M. Chapman Wilbert, J. Pellegrino, A. Zydney, Bench scale testing of surfactant-modified reverse osmosis/nanofiltration membranes, Desalination 115 (1998) 15–32.

[5] M. Nyström, L. Kaipia, S. Luque, Fouling and retention of nanofiltration membranes, J. Membr. Sci. 98 (1995) 249–262.

[6] D. Möckel, E. Staude, M. Dal-Cin, K. Darcovich, M. Guiver, Tangential flow streaming potential measurements: Hydrodynamic cell characterization and zeta potentials of carboxylated polysulfone membranes, J. Membr. Sci. 145 (1998) 211–222.

[7] G.B. Westermann-Clark, J.L. Anderson, Experimental verification of the space-charge model for electrokinetics in charged microporous membranes, J. Electrochem. Soc., Electrochem. Sci Technol. 130 (1983) 839–847.

[8] W.H. Keesom, R.L. Zelenka, C.J. Radke, A zeta-potential model for ionic surfactant adsorption on an ionogenic hydrophobic surface, J. Colloid Interface Sci. 125 (1988) 575–585.

[9] M. Nystrom, M. Lindstrom, E. Matthiasson, Streaming potential as a tool in the characterization of ultrafiltration membranes, Colloids Surf. 36 (1989) 297–312.

[10] K.J. Kim, A.G. Fane, M. Nystrom, A. Pihlajamaki, W.R. Bowen, H. Mukhtar, Evaluation of electroosmosis and streaming potential for measureement of electric charges of polymeric membranes, J. Membr. Sci. 116 (1996) 149–159.

[11] M. Elimelech, A. Childress, Zeta potential of reverse osmosis membranes: implications for membrane performance, Water Treatment Technology Program Report No. 10, US Bureau of Reclamation, 1996.

[12] A.E. Childress, M. Elimelech, Effect of solution chemistry on the surface charge of polymeric reverse osmosis and nanofiltration membranes, J. Membr. Sci. 119 (1996) 253–268.

[13] A. Szymczyk, P. Fievet, J.C. Reggiani, J. Pagetti, Characterisation of surface properties of ceramic membranes by streaming and membrane potentials, J. Membr. Sci. 146 (1998) 277–284.

[14] P.C. Hiemenz, Principles of Colloid and Surface Chemistry, 3rd ed., Dekker, New York, 1997.

[15] R.J. Hunter, Introduction to Modern Colloid Science, Oxford University Press, Oxford, 1996.

[16] M. Elimelech, J. Gregory, X. Jia, R.A. Williams, Particle Deposition and Aggregation: Measurement, Modelling and Simulation, Butterworth Heinemann, Oxford, 1995.

[17] F. Fairbrother, H. Mastin, J. Chem. Soc. 75 (1924) 2318.

[18] G.P. Box, W.G. Hunter, J.S. Hunter, Statistics for Experimenters: An Introduction to Design, Data Analysis and Model Building, Wiley, New York, 1978.